

Article

Solar Radiation Forecasting Using Machine Learning and Ensemble Feature Selection

Edna S. Solano ^{1,*}, Payman Dehghanian ² and Carolina M. Affonso ¹¹ Faculty of Electrical Engineering, Federal University of Para, Belem 66075-110, PA, Brazil² Department of Electrical and Computer Engineering, The George Washington University, Washington, DC 20052, USA

* Correspondence: edna.solano@unah.edu.hk

Abstract: Accurate solar radiation forecasting is essential to operate power systems safely under high shares of photovoltaic generation. This paper compares the performance of several machine learning algorithms for solar radiation forecasting using endogenous and exogenous inputs and proposes an ensemble feature selection method to choose not only the most related input parameters but also their past observations values. The machine learning algorithms used are: Support Vector Regression (SVR), Extreme Gradient Boosting (XGBT), Categorical Boosting (CatBoost) and Voting-Average (VOA), which integrates SVR, XGBT and CatBoost. The proposed ensemble feature selection is based on Pearson coefficient, random forest, mutual information and relief. Prediction accuracy is evaluated based on several metrics using a real database from Salvador, Brazil. Different prediction time-horizons are considered: 1 h, 2 h and 3 h ahead. Numerical results demonstrate that the proposed ensemble feature selection approach improves forecasting accuracy and that VOA performs better than the other algorithms in all prediction time horizons.

Keywords: ensemble feature selection; machine learning; photovoltaic generation; solar radiation forecasting

Citation: Solano, E.S.; Dehghanian, P.; Affonso, C.M. Solar Radiation Forecasting Using Machine Learning and Ensemble Feature Selection. *Energies* **2022**, *15*, 7049. <https://doi.org/10.3390/en15197049>

Academic Editors: Pei Du, Tong Niu and Mingjian Cui

Received: 25 August 2022

Accepted: 22 September 2022

Published: 25 September 2022

Publisher's Note: MDPI stays neutral with regard to jurisdictional claims in published maps and institutional affiliations.



Copyright: © 2022 by the authors. Licensee MDPI, Basel, Switzerland. This article is an open access article distributed under the terms and conditions of the Creative Commons Attribution (CC BY) license (<https://creativecommons.org/licenses/by/4.0/>).

1. Introduction

Solar generation is a clean renewable energy resource that has emerged as a promising solution for reducing fossil fuel consumption and CO₂ emissions. According to [1], solar energy continued globally to lead renewable capacity expansion with an increment of 133 GW (+19%) in 2021, achieving a total of 849 GW capacity and accounting for 28% of the renewable generation portfolio.

The operation of power systems with high penetration of photovoltaic (PV) generation brings about some challenges due to its non-dispatchability and intermittence, dependent on meteorological parameters and mainly cloud dynamics. The fluctuating PV generation may lead to power flow inversion with voltage and frequency variations and an imbalance between energy demand and supply; therefore, it requires the development of accurate solar radiation forecasting models for reliable power system operation.

Several forecasting models have been proposed in the literature targeting different prediction time horizons: very short-term (intra-hour), short-term (intra-day or day-ahead), medium-term (1 month) and long-term (1 year) [2], each driving different applications. For example, intra-hour and intra-day forecasting can be used for real-time power system operation. Day-ahead forecasting can be used for dispatch planning purposes. Medium and long-term forecasts can be used for maintenance and energy market purposes. Forecasting algorithms can be classified into physical models, such as Numerical Weather Prediction (NWP); statistical models, such as Autoregressive Moving Average (ARMA) and Autoregressive Integrated Moving Average (ARIMA); and data-driven models, such as Artificial Intelligence (AI) algorithms.

Physical models are based on sky images, satellite information, and mathematical equations that requires in depth understanding to describe the physical phenomena in the atmosphere [3]. Statistical models had been widely used in early works to forecast solar radiation with satisfactory results. In [4], ARMA and ARIMA models are used for short-term solar radiation forecasting. In [5], authors propose to combine an autoregressive (AR) model with a dynamical system model to 1 h-ahead solar radiation forecasting.

Over time, these models have been outperformed by techniques belonging to the field of artificial intelligence (AI) due to their ability to detect nonlinear relationships [6]. Several papers have been developed to forecast solar radiation using AI algorithms. In [7], authors compare the performance of regression and Artificial Neural Network (ANN) models to forecast solar radiation, and results show that ANN outperforms regression models. Reference [8] proposes the use of a genetic algorithm to adjust ANN parameters on a solar power forecasting model. The results are compared with ARIMA and ANN and show substantial improvements can be achieved with genetic algorithm optimization. Reference [9] proposes a hybrid model to forecast hourly solar irradiance based on self-organizing maps (SOM), support vector regression (SVR) and particle swarm optimization (PSO), and the proposed technique outperforms traditional forecasting models. More recently, researchers have used machine learning (ML) techniques to forecast solar radiation, which is a promising subfield of AI capable of dealing with a large amount of data [10]. The ML algorithms most commonly found in the literature are: support vector regression (SVR), regression tree, random forest and gradient boosting.

The forecasting model can be constructed using only endogenous inputs or with both endogenous and exogenous inputs. The endogenous input is the solar radiation time series itself, and the exogenous inputs can be the meteorological parameters that most affect the prediction, such as air temperature, humidity, wind speed, wind direction, and atmospheric pressure. A review of some recent literature on solar radiation forecasting indicates that researchers have primarily focused on developing new models and hybridizing different ML algorithms to improve forecast accuracy, mostly using as inputs past observations of solar radiation. For instance, reference [11] applies a deep learning model for solar radiation forecasting with a time horizon of 10 min and uses as input only historical observations of solar radiation. In [12], the authors propose a hybrid model for short-term solar irradiance prediction combining Long Short-Term-Memory (LSTM) and a Convolutional Neural Network (CNN), using as input the solar irradiance historical series. Reference [13] investigates the use of various deep neural network models for the one-day-ahead prediction of global horizontal irradiation (GHI) in Saudi Arabia, using only the historical values of daily GHI.

The high correlation between solar radiation and some meteorological parameters encouraged authors to use both endogenous and exogenous inputs to improve solar radiation forecasting accuracy. However, most of them perform the selection of exogenous inputs using limited algorithms such as Pearson's correlation coefficient, which only identifies linear relationships between variables or, intuitively, by trying different combinations of input variables and choosing the one that gives the minimum forecasting error. Reference [14] proposes a solar irradiance prediction model using LSTM for three prediction horizons (1, 15 and 60 min). Two sets of input variables are considered: a complete dataset with seven meteorological data and a reduced dataset with only three meteorological data. However, the authors do not apply a feature selection methodology to adequately choose the most significant inputs. In [15], the authors propose an ensemble model for short-term PV generation forecasting combining Extreme Learning Machines (ELM), Extremely Randomized Trees (ET), k-Nearest Neighbor (KNN), Mondrian Forest (MF) and a Deep Belief Network (DBN). Several meteorological data are used as input in the forecasting model. However, the authors do not employ an input selection methodology. Reference [16] evaluates the performance of different ML algorithms for PV generation forecasting such as Linear Regression (LR), Polynomial Regression (PR), Decision Tree (DT), Support Vector Regression (SVR), Random Forest (RF), LSTM, and Multilayer

Perceptron (MLP). Some meteorological parameters are used in the forecasting model, and different forecast time horizons are considered (24-h, 1 week and 1 year). In this study, input selection is performed intuitively, analyzing the relationship between each exogenous variable and the output variable.

Few studies apply a feature selection methodology for solar radiation forecasting. Reference [17] investigates the effectiveness of using exogenous inputs to perform short-term GHI forecasting with several ML models. The authors applied the following feature selection techniques: correlation, information, sequential forward selection, sequential backward selection, LASSO regression, and random forest. In [18], the authors use a hybrid ML model to perform PV power forecasting with an enhanced forward selection based on a Light Gradient Boosting decision tree (LightGBDT). In both papers, the results show that exogenous inputs improve forecasting performance.

In addition to the selection of exogenous inputs, the selection of the most related delay values (past observations) plays a key role in ensuring an effective prediction [19]. Each feature may have a temporal effect on solar radiation. For instance, some features may have a greater impact on more recent past observations, while other features may only have an impact on more distant past observations. Therefore, it is necessary to find the most relevant features and their corresponding delay value.

Few researchers have explored the optimal selection of input delay values in the solar radiation forecasting problem. This paper tries to address this knowledge gap in the literature by proposing a forecasting methodology using ML models which incorporates exogenous information and an ensemble feature selection method with an in-depth analysis to choose not only input parameters but also their delay values. The performance of several ML algorithms is investigated, and a comparative analysis is presented considering different prediction time-horizons. The ML-implemented algorithms are: Support Vector Regression (SVR), Extreme Gradient Boosting (XGB), Categorical Boosting (CatBoost) and Voting-Average (VOA). The ensemble feature selection is based on Pearson's coefficient, random forest, mutual Information and relief. Prediction accuracy is assessed based on several evaluation metrics. The proposed methods are tested with a real database from Salvador, Brazil.

The key contributions of this study are highlighted as follows:

- Comparing the performance of different state-of-the-art ML algorithms, including the CatBoost algorithm, which presents fewer applications in solar radiation forecasting to the best of the authors' knowledge;
- Proposing an ensemble feature selection method to select the most significant endogenous and exogenous variables and their delay values, integrating different ML algorithms.

2. Proposed Methodology

The proposed approach for solar radiation forecasting includes five main steps and is presented in Figure 1. First, a real and substantial database is obtained containing data on solar radiation and other meteorological information. Then, pre-processing is performed to clean the data by removing outliers and imputing missing values. Normalization is also applied to avoid biasing toward extreme values. The next step is to select the most significant variables and their delay values, using an ensemble feature selection combining Pearson's correlation coefficient, random forest, mutual information and relief. Then, data is separated into training, validation and test sets, and different machine learning algorithms are applied. Finally, various statistical indicators are used to quantify the accuracy of the forecasting algorithms.

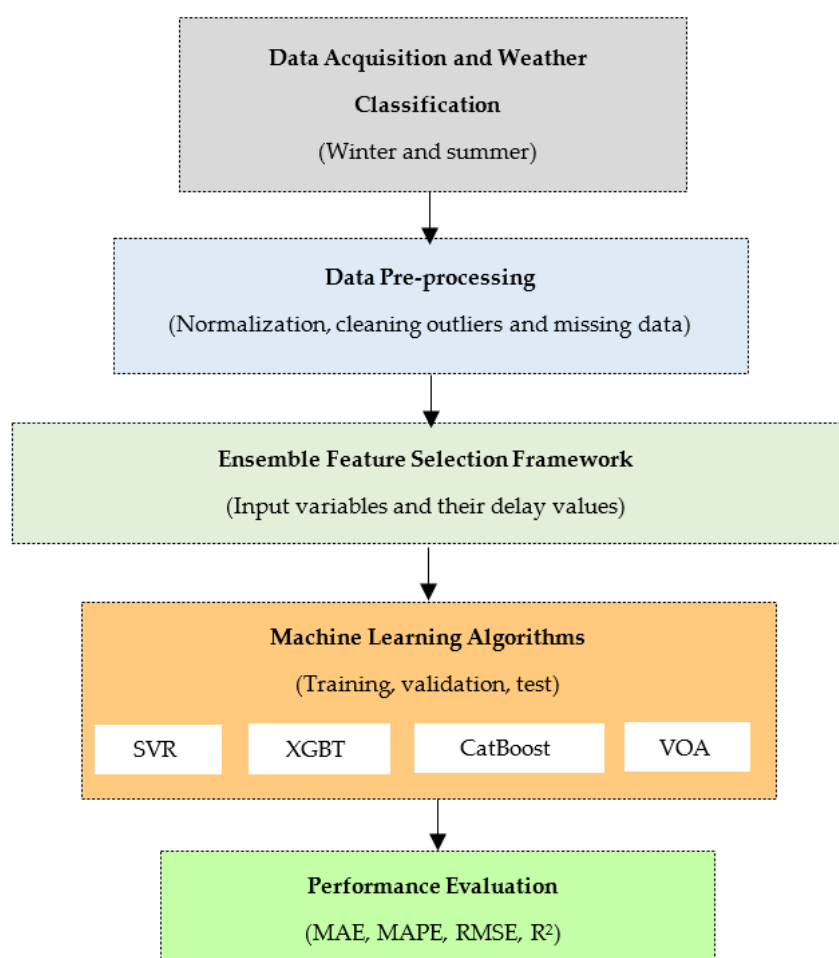


Figure 1. Flowchart of the proposed methodology.

2.1. Data Description

Simulations are conducted using real-world data collected from the Brazilian National Institute of Meteorology website (INMET), which provides data from several weather stations in Brazil [20]. The referred data is from the city of Salvador, Brazil ($12^{\circ}58'28.9992''$ S, $38^{\circ}28'35.9940''$ W), with hot and rainy weather all year round. Temperatures are quite stable with a minimum of 22°C and a maximum of 31°C . The period covered by the database is from 1 January 2015 to 3 August 2021 in sampling intervals of 1 h. Table 1 shows all variables in the database, and their statistical analysis is presented in Table 2.

Table 1. Available database for solar radiation forecasting.

Data	Abbreviation	Unity
Hour	H	hour
Global solar radiation	R	MJ/m^2
Maximum wind gust	W_g	m/s
Wind speed	W_s	m/s
Wind direction	W_d	$^{\circ}$
Dry bulb temperature	T	$^{\circ}\text{C}$
Hourly maximum temperature	T^{\max}	$^{\circ}\text{C}$
Hourly minimum temperature	T^{\min}	$^{\circ}\text{C}$
Dew point temperature	T_d	$^{\circ}\text{C}$

Hourly maximum dew point temperature	T_{d}^{\max}	°C
Hourly minimum dew point temperature	T_{d}^{\min}	°C
Total precipitation	P	mm
Station atmospheric pressure	A	mb
Hourly maximum atmospheric pressure	A^{\max}	mb
Hourly minimum atmospheric pressure	A^{\min}	mb
Relative humidity	H	%
Hourly maximum relative humidity	H^{\max}	%
Hourly minimum relative humidity	H^{\min}	%

Table 2. Statistical features of the available database.

Variable	Mean	Standard Deviation	Min	Max
H	12.0	3.1623	7.0	17.0
R	1.6533	1.0462	0.0009	4.15
W_g	5.6651	1.7302	0.6000	10.6
W_s	1.6069	0.5372	0.1	3.0
W_d	130.8017	59.7526	1.0	360.0
T	27.3608	2.4069	20.4	34.2
T^{\max}	28.1414	2.5181	20.8	35.8
T^{\min}	26.5007	2.3708	19.9	32.4
T_d	21.5368	1.4812	16.8	25.5
T_d^{\max}	22.2897	1.4708	17.3	26.0
T_d^{\min}	20.8531	1.4820	16.3	25.1
P	0.2041	1.3419	0.0	50.4
A	1009.4062	2.9636	1001.6	1017.7
A^{\max}	1009.7137	2.9276	1001.9	1018.1
A^{\min}	1009.2102	2.9265	1001.4	1017.5
H	71.3240	10.4711	45.0	96.0
H^{\max}	75.0566	10.1359	52.0	97.0
H^{\min}	68.1149	11.0133	38.0	96.0

Figure 2 shows the average monthly solar radiation. The dataset is divided into two periods according to the stable weather condition of the city, and different forecasting models are developed for each period. These periods are summer, from September to March, and winter, from April to August. The forecasting methodology and algorithms are implemented using Jupyter and Scikit-Learn libraries.

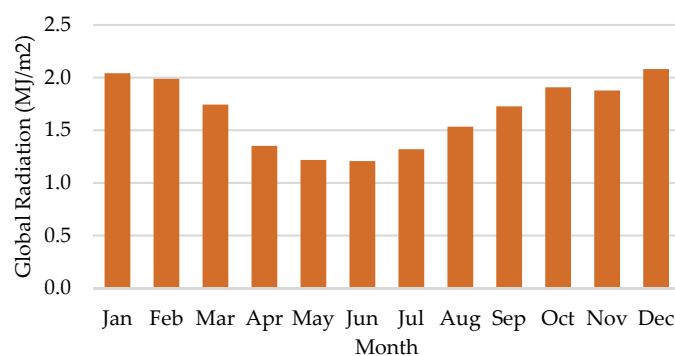


Figure 2. Average monthly solar radiation from January 2015 to August 2021 in Salvador, Brazil.

2.2. Pre-Processing

The pre-processing data is an important step to achieve an accurate forecasting model. First, the data needs to be cleaned from inconsistent measurements, such as missing data points and outliers [21]. In solar radiation times series, only daytime samples are considered. If the complete time series is used, many observed values are zero (night period), and the forecast values will also be zero (or very close), substantially reducing the prediction error and overestimating the performance of the forecasting model. In the other time series, missing values are replaced by applying imputation through the interpolation of the observed values. Outliers are detected using the Interquartile Range (IQR) method, which divides an ordered dataset into four quartiles (Q_1 , Q_2 , Q_3 , Q_4), each quartile containing 25% of the data. The IQR is evaluated as the difference between Q_3 and Q_1 , and outliers are defined as observations that fall below $Q_1 - 1.5 \times \text{IQR}$ or above $Q_3 + 1.5 \times \text{IQR}$. After being identified, outliers are treated by applying interpolation, since the exclusion of these records would considerably reduce the size of the available data and affect the continuity of the hourly sampling. Min-max normalization is further applied to scale data into $[0, 1]$.

The historical dataset is divided into three sets: training, validation and testing. The training set is used to build the ML model, with known inputs and outputs. The validation set is used to fine-tune the model hyperparameters. The testing set is used to estimate the model performance on data not used to train the model. The training set covers 70% of data with 18,521 registers from 2015 to 2019; the validation set covers 10% of data with 2629 registers from 2019 to 2020, and the test set covers 20% of data with 5299 registers from 2020, as shown in Figure 3. The validation and training sets are not continuous due to data splitting according to summer and winter seasons.

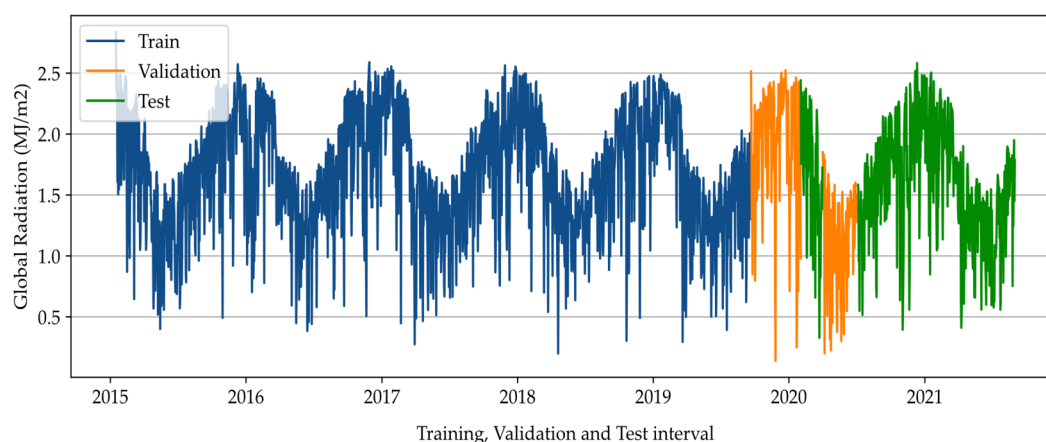


Figure 3. Training, validation and testing set of solar radiation historical series.

2.3. Ensemble Feature Selection

Feature selection is commonly applied in machine learning algorithms to select the best set of variables that represent the original data, thus reducing data size and model complexity and improving prediction performance [22]. Different feature selection algorithms are often tested, and the variable set with the best forecasting performance is chosen. Alternatively, an ensemble feature selection can be applied by aggregating several feature selection algorithms, combining the advantages of each one. The proposed methodology is presented in Figure 4.

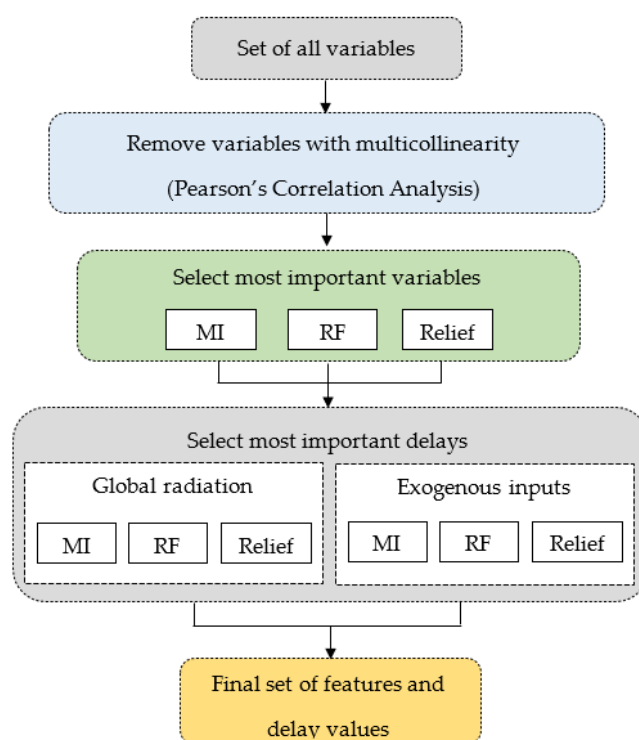


Figure 4. Ensemble feature selection methodology.

The dataset used in this paper is composed of solar radiation historical series as the endogenous variable (values determined by the model) and other meteorological variables as exogenous variables (values determined outside the model). Feature selection is applied to choose the most important exogenous variables and delay values, analyzing both linear and non-linear relationships among features.

First, Pearson's correlation analysis is performed [21]. Figure 5 shows the correlation matrix between exogenous variables for winter (a) and summer (b) seasons. A correlation coefficient $r = 0$ indicates that no linear relationship exists between variables, and the relationship becomes stronger as r approaches -1 or $+1$. As expected, results indicate a high linear correlation between variables and their minimum and maximum values. Accordingly, the following variables are removed from the dataset: hourly maximum and minimum atmospheric pressure, hourly maximum and minimum temperature, hourly maximum and minimum dew point temperature, and hourly maximum and minimum relative humidity.

An ensemble feature selection is next applied to select the most significant variables integrating the following algorithms: Mutual Information (MI), Random Forest (RF) and relief [23–25]. For each method, the importance of each variable is evaluated, and its value is further normalized. The final variable importance ranking is achieved by computing the mean value from different feature selection methods. The most important variables are global radiation, dry bulb temperature, relative humidity, wind speed, atmospheric pressure, and time. The threshold between the selected features and the discarded features was found empirically during the model optimization phase.

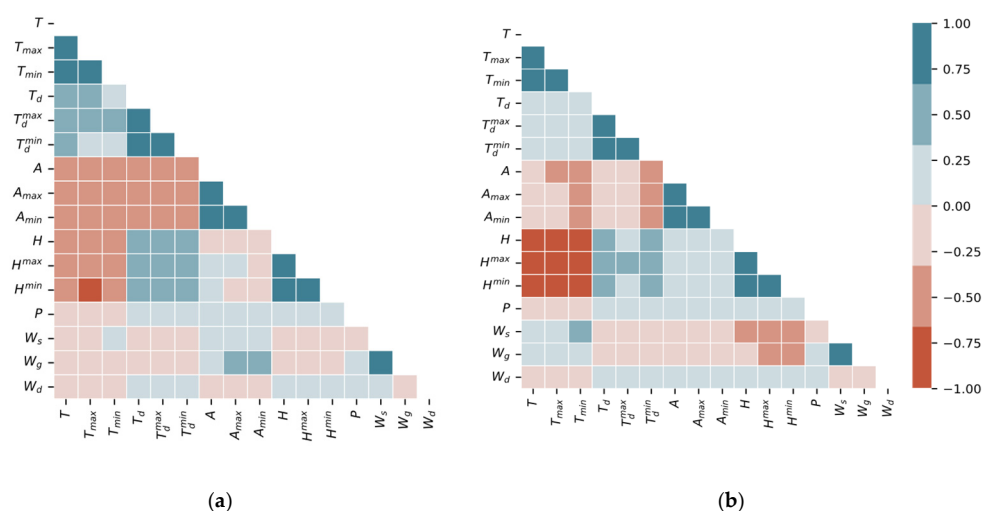


Figure 5. Correlation matrix: (a) winter season and (b) summer season.

Since the dataset consists of multivariate time series, the proper selection of variable delays (past observations) is an important task to ensure acceptable forecasting accuracy. The next step is to select the delays of the endogenous and exogenous variables applying the same ensemble model. The selection of the most significant lags for the exogenous variables is done separately from the endogenous variable since they have a reduced but no weaker significance. Considering $X_t - k$, a delay of k hours in variable X , the adopted range of delays to be tested is from 1 to 72 for each variable ($X_{t-1} \dots X_{t-72}$), which seemed sufficient to capture important information from historical values. The final dataset with the selected variables and their delays is listed in Table 3.

Table 3. Selected set of input variables and delay values.

Winter	
Variable	Delays
Global solar radiation	$t-1, t-2, t-23, t-24, t-25, t-47, t-48, t-72$
Dry bulb temperature	$t-1, t-2, t-23, t-24, t-25, t-48, t-49, t-72$
Relative humidity	$t-1, t-2, t-23, t-24, t-25, t-48, t-49, t-72$
Wind speed	$t-1, t-24$
Atmospheric pressure	$t-2$
Hour, day, month	-
Summer	
Variable	Delays
Global solar radiation	$t-1, t-2, t-23, t-24, t-25, t-47, t-48, t-72$
Dry bulb temperature	$t-1, t-2, t-23, t-24, t-25, t-48, t-49, t-72$
Relative humidity	$t-1, t-2, t-23, t-24, t-25, t-48, t-49, t-72$
Wind speed	$t-1, t-2$
Atmospheric pressure	$t-3$
Hour, day, month	-

3. Machine Learning Algorithms

The performance of several ML algorithms is evaluated to predict solar radiation applying the proposed methodology. The algorithms used are SVR, XGBT, CatBoost and VOA, which are briefly presented below.

3.1. Support Vector Regression (SVR)

Support Vector Regression (SVR) is an extension to the Support Vector Machine (SVM) algorithm applied to regression (predicting a continuous quantity output) instead

of classification problems [26]. In basic regression models, the error is minimized, while it is fitted in SVR within a certain threshold (ϵ) around the regression line (hyperplane), such that all data points within ϵ are not penalized for their error.

The problem can be formulated as follows:

$$\begin{aligned} & \text{Min. } \frac{1}{2} \|w\|^2 + C \sum_{i=1}^n |\xi_i| \\ \text{s. a. } & |y_i - w_i x_i| \leq \epsilon + |\xi_i| \quad i = 1, 2, \dots, n \end{aligned} \quad (1)$$

where n is the number of training samples, the slack variable ξ is the deviation for any value that falls outside ϵ , and C is the penalty factor that determines the tradeoff between minimizing the training error and minimizing model complexity. As C increases, the tolerance for points outside ϵ also increases. The performance of SVR then depends on the choice of parameters ϵ and C .

3.2. Extreme Gradient Boosting (XGBoost)

Extreme gradient boosting is a decision-tree based ensemble algorithm that improves the performance of weak learners to establish an effective joint model [27]. This algorithm uses a tree ensemble model, shown in Figure 6, to predict the output.

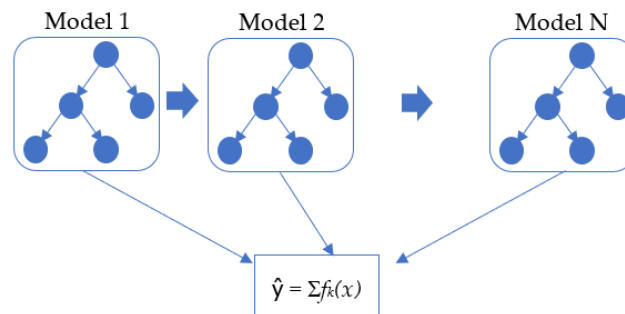


Figure 6. Tree ensemble model for boosting algorithms.

It has been widely applied to many problems with success. In boosting, the trees are built sequentially such that each subsequent tree learns and reduces the errors of the previous one. A gradient descending algorithm is employed to minimize errors when adding new models. XGBoost uses parallel processing, considerably improving the training time. It is important to mention that XGBoost has a large range of hyperparameters, and their appropriate tuning is critical to the algorithm's performance.

3.3. Categorical Boosting (CatBoost)

CatBoost is a gradient boosting framework developed by Prokhorenkova et al. [28] in 2017 and uses a binary decision-tree as base predictors. CatBoost has two main differences compared with other boosting algorithms. It uses the concept of ordered boosting, which is a random permutation approach to train the model with a subset of data while calculating residuals with another subset, thus preventing overfitting. Furthermore, the same splitting criterion is used at all nodes creating always symmetric trees. These trees are balanced and less prone to overfitting, which significantly speeds up the model execution. The CatBoost is, however, sensitive to hyperparameter tuning.

3.4. Voting Average (VOA)

Voting-averaged is an ensemble algorithm that combines the prediction from multiple ML algorithms [29]. In regression problems, VOA takes the predictions of each model and computes their average value to derive a final prediction. By combining different models, the risk of having a poor performance from one model can be mitigated by the strong performance from the other models, achieving a more robust algorithm. Since

voting uses multiple ML algorithms, it is more computationally intensive. In this paper, VOA is implemented by combining: SVR, XGBT and CatBoost.

4. Performance Metrics

The performance of the algorithms is evaluated using the following error metrics: mean absolute error, mean absolute percentage error, and root mean square error. The lower the measures, the better the prediction. In the following equations, F_i is the forecasted value, O_i is the observed value, \bar{O}_i is the mean value of observations, and n is the number of samples.

Mean absolute error (MAE):

$$\text{MAE} = \frac{1}{n} \sum_{i=1}^n |F_i - O_i| \quad (2)$$

Mean absolute percentage error (MAPE):

$$\text{MAPE} = \frac{1}{n} \sum_{i=1}^n \left| \frac{F_i - O_i}{O_i} \right| \times 100 \quad (3)$$

Root mean square error (RMSE):

$$\text{RMSE} = \sqrt{\frac{1}{n} \sum_{i=1}^n (F_i - O_i)^2} \quad (4)$$

The coefficient of determination (R^2) is also evaluated. It measures the variance in the predictions and varies from 0 to 1. A coefficient equal to 1 indicates that the model perfectly interprets the observed data, while a 0 indicates the model predictions perform badly on unseen data. The coefficient of determination is evaluated as follows:

$$R^2 = 1 - \frac{\sum_{i=1}^n (F_i - O_i)^2}{\sum_{i=1}^n (F_i - \bar{O}_i)^2}, \quad \bar{O}_i = \sum_{i=0}^{n-1} F_i \quad (5)$$

In addition, statistical moments such as skewness (SK) and kurtosis (K) are evaluated. Skewness is a statistical measure of the asymmetry of the error distribution. It indicates the overall tendency of a forecasting model to over-forecast (in case of positive skewness) or under-forecast (in case of negative skewness). Kurtosis is a statistical measure that assesses the propensity of a distribution to have extreme (outliers) values within its tails. The excess kurtosis is a form to compare to Gaussian distribution. Since Gaussian distribution has a kurtosis of 3, excess kurtosis is evaluated by subtracting kurtosis by 3. Positive values of excess kurtosis indicate that the distribution tail is heavier and longer than Gaussian distribution, with a probability of containing more extreme values (outliers). Negative values of excess kurtosis indicate that the distribution has light tails that are shorter than Gaussian distribution and include fewer extreme values.

5. Results and Discussion

This section presents the results obtained with the proposed methodology using several ML algorithms for solar forecasting under different temporal scales. The relevance of performing an ensemble feature selection is also investigated. The hyperparameters adopted in the algorithms were selected using the GridSearchCV function from Scikit learn library [30]. It is a grid search technique that exhaustively enumerates all hyperparameter combinations and evaluates the accuracy of each combination through the validation set. Hyperparameters for both forecasting models are presented in Table 4.

Table 4. Algorithm hyperparameter tuning.

Algorithm	Hyperparameter	
	Winter	Summer
SVR	regularization C = 10, ϵ = 0.01, γ = auto, kernel function K = RBF	Regularization C = 100, ϵ = 0.001, γ = auto, kernel function K = RBF
XGBT	learning rate = 0.1, max. depth = 5, number of estimators = 80, subsample = 0.9	learning rate = 0.1, max. depth = 5, number of estimators = 100, subsample = 0.8
CatBoost	depth = 6, L2 regularization = 10, learning rate = 0.05, iterations = 2000	depth = 6, L2 regularization = 10, learning rate = 0.05, iterations = 2000
VOA	XGBT (learning rate = 0.1, max. depth = 5, number of estimators = 80, subsample = 0.9)	XGBT (learning rate = 0.1, max. depth = 5, number of estimators = 100, subsample = 0.8)
	CatBoost (depth = 6, L2 regularization = 10, learning rate = 0.05, iterations = 2000)	CatBoost (depth = 6, L2 regularization = 10, learning rate = 0.05, iterations = 2000)
	SVR (regularization C = 10, ϵ = 0.01, γ = auto, kernel function K = RBF)	SVR (regularization C = 100, ϵ = 0.001, γ = auto, kernel function K = RBF)

5.1. Impact of Feature Selection of Variables and Delays

In this section, the effectiveness of using an ensemble feature selection for solar radiation forecasting is investigated. Two other cases are analyzed for comparison purposes:

- Case 1: The forecasting model is trained using only endogenous inputs, which is the solar radiation and its 10 past observations;
- Case 2: The forecasting model is trained using both endogenous and exogenous inputs (solar radiation and other meteorological data), and their past observations are selected using the Pearson correlation coefficient;
- Case 3: The forecasting model is trained using both endogenous and exogenous inputs, selected using the proposed ensemble feature selection.

The algorithm to perform this analysis is VOA, and for a fair comparison, the hyperparameters are kept the same in the three cases, and the models are trained and tested using the same dataset partition from the training set only. The results are presented in Table 5. Among all of them, Case 3 shows better prediction accuracy using all metrics.

Table 5. Comparison of forecasting performance for different input datasets using VOA.

Winter				
Input Set	MAE	RMSE	MAPE	R ²
Case 1: endogenous	0.2591	0.3532	34.1955	0.8377
Case 2: end + exog (Pearson coefficient)	0.2521	0.3439	32.8627	0.8460
Case 3: endo + exog (ensemble selection)	0.2537	0.3431	31.8928	0.8468
Summer				
Input Set	MAE	RMSE	MAPE	R ²
Case 1: endogenous	0.3153	0.4536	35.4139	0.8261
Case 2: end + exog (Pearson correlation)	0.3017	0.4358	31.1411	0.8395
Case 3: endogenous and exogenous	0.303	0.4326	30.6106	0.8417

Figure 7 shows the learning curve obtained with VOA for all cases. The learning curve shows the relationship between training and validation errors with a variable number of training samples. Through its analysis, it is possible to diagnose bias and variance problems in supervised learning models. In all cases, as the size of the training set increases, the training error increases and the validation error decreases, converging for a small error value, which is the desirable behavior. The narrow gap between the training and validation curves indicates a low variance error. Training data are fitted well, and the algorithm can generalize on unseen data. Case 3 has lower training and validation errors. This highlights the positive impact of applying the proposed ensemble feature and delays the selection method, which keeps the features and their significant delays that provide

the most relevant information and discards features and delays that may be negatively impacting the learning process.

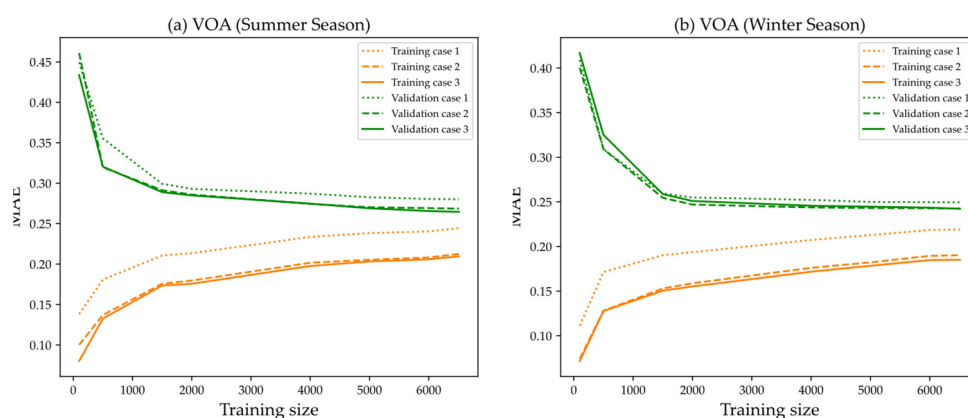


Figure 7. Learning Curves for VOA. (a) Summer season. (b) Winter season.

5.2. Forecasting Accuracy of Machine Learning Algorithms

This section compares the results obtained using four different ML algorithms for solar radiation forecasting with a 1-hour-ahead prediction horizon. The proposed ensemble feature selection with endogenous and exogenous inputs is applied in all cases. Table 6 shows the forecasting accuracy for the test dataset in terms of MAE, RMSE, MAPE, R^2 , SK and K. VOA showed the best predictive performance in all metrics, except for MAPE, wherein CatBoost has a slightly lower error. XGBoost presented the worst performance for all metrics during winter and summer. All models have low and positive skewness values, implying that they are more likely to forecast radiance values above rather than below the mean value. Furthermore, except for SVR during the summer season, all models exhibit negative excess kurtosis, indicating that the models are less likely to deliver extreme prediction errors.

Table 6. Forecasting accuracy of ML algorithms (1 h ahead).

Winter				
	SVR	XGBoost	CatBoost	VOA
MAE	0.2430	0.2534	0.2426	0.2417
RMSE	0.3433	0.3507	0.3470	0.3418
MAPE	28.0122	29.5350	27.2163	27.4862
R^2	0.8466	0.8399	0.8433	0.8480
SK	0.1336	0.0880	0.0994	0.1039
K	−1.1632	−1.1829	−1.2022	−1.1877
Summer				
	SVR	XGBoost	CatBoost	VOA
MAE	0.2922	0.3009	0.2905	0.2877
RMSE	0.4366	0.4426	0.4373	0.4309
MAPE	28.3590	28.6951	26.8127	27.3177
R^2	0.8389	0.8344	0.8383	0.8430
SK	0.0462	0.0332	0.0338	0.0360
K	0.2922	−1.1663	−1.1551	−1.1563

Figure 8 shows the histogram of absolute errors obtained with each algorithm. The number of records is displayed at the top of each bin. It is possible to see that all of the ML algorithms exhibit a similar histogram. In all cases, the peak of each error distribution is centered around zero, showing that the most likely occurrence is a small solar radiation forecast error.

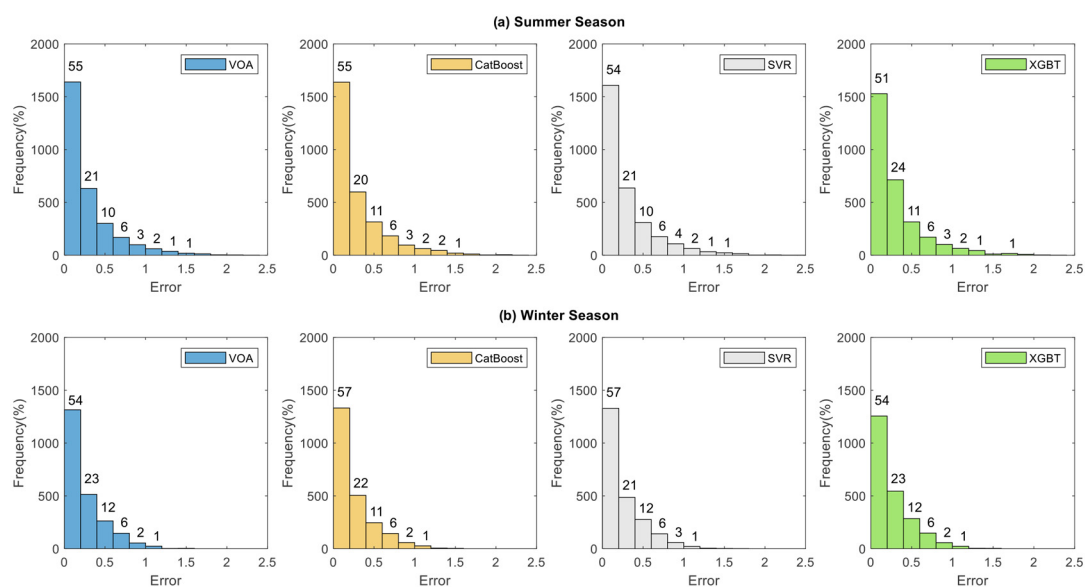
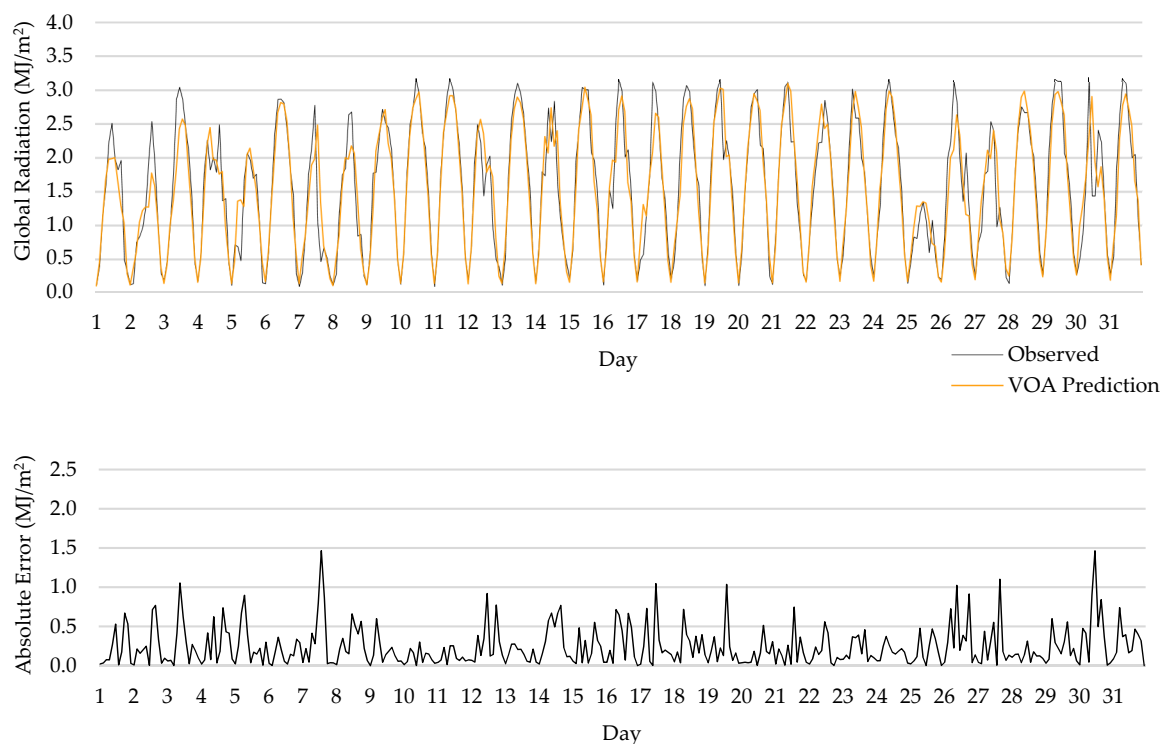
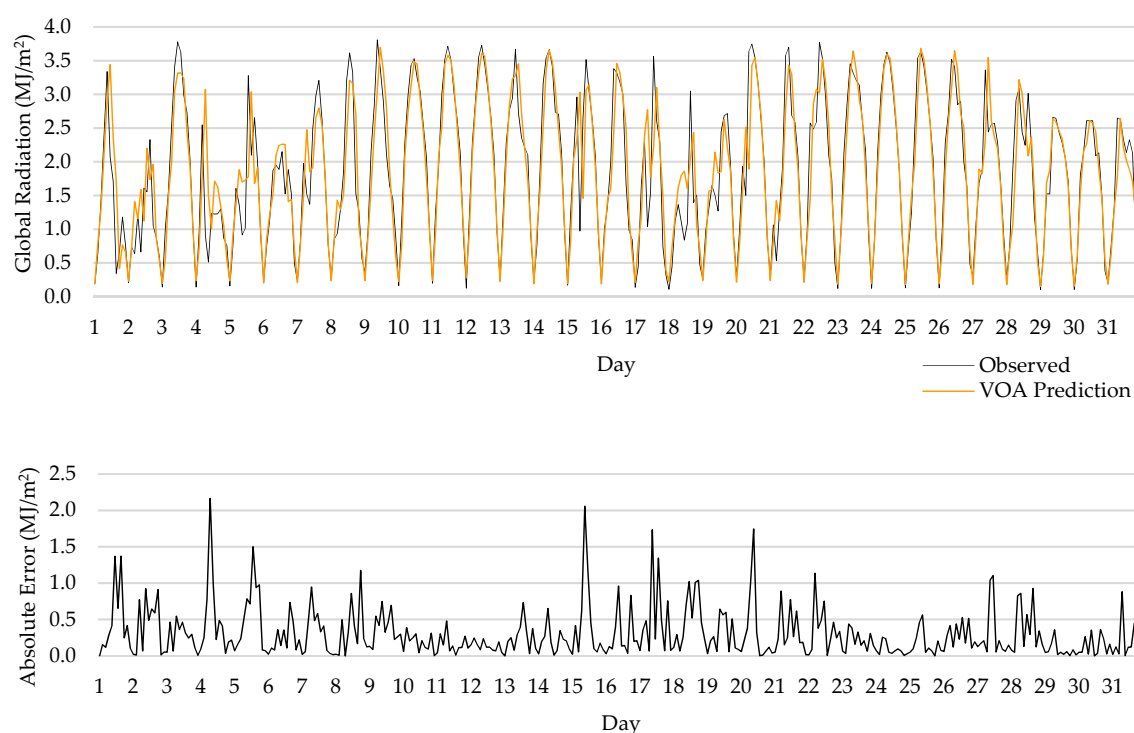


Figure 8. Histogram of the absolute error for all ML algorithms. (a) Summer. (b) Winter.

Figure 9 shows the solar radiation observed, forecast and the residuals obtained with the VOA algorithm during the months of winter and summer seasons, respectively. The forecasting error is larger in summer than in winter.



(a) Winter (August 2021)



(b) Summer (February 2021)

Figure 9. Solar radiation observed, forecast and residuals for 1 h ahead using VOA: (a) winter and (b) summer.

It is important to evaluate the computational performance of the algorithm when dealing with real-world applications. Table 7 shows the learning speed in seconds for all algorithms using summer and winter datasets, averaged over 20 runs. All of the experiments were performed on a computer with an Intel i5-1035G1 CPU (1.19 GHz) and 8.0 GByte RAM. XGBT has the lower training speed for summer and winter datasets, 2.85 s and 1.75 s, respectively. VOA has the higher training speed for summer and winter datasets, 183.93 s and 14.76 s. VOA combines SVR, XGBT and CatBoost, being more complex. All ML algorithms have a higher training speed for the summer dataset because it has more registers (data from September to March) than the winter dataset (data from April to August). All algorithms have an acceptable testing speed, with an average execution computational time of 11 s.

Table 7. Average learning speed in seconds (s) for all ML algorithms (1 h ahead).

Learning Speed (s)				
	SVR	XGBT	CatBoost	VOA
Summer	63.09	2.85	13.08	183.93
Winter	9.73	1.75	9.81	14.76
Testing Speed (s)				
Summer	36.99	1.44	13.35	13.14
Winter	4.91	1.17	10.27	10.58

5.3. Results for Different Temporal Scales

The variability and stochasticity of photovoltaic generation usually occur on ultra-short-term and short-term time scales. Therefore, it is important to compare the effectiveness of the forecasting methodology under different temporal scales. Figure 10 shows the

MAE, RMSE, MAPE and R^2 for all algorithms, considering three forecasting horizons: 1 hour ahead, 2 hours ahead, and 3 hours ahead.

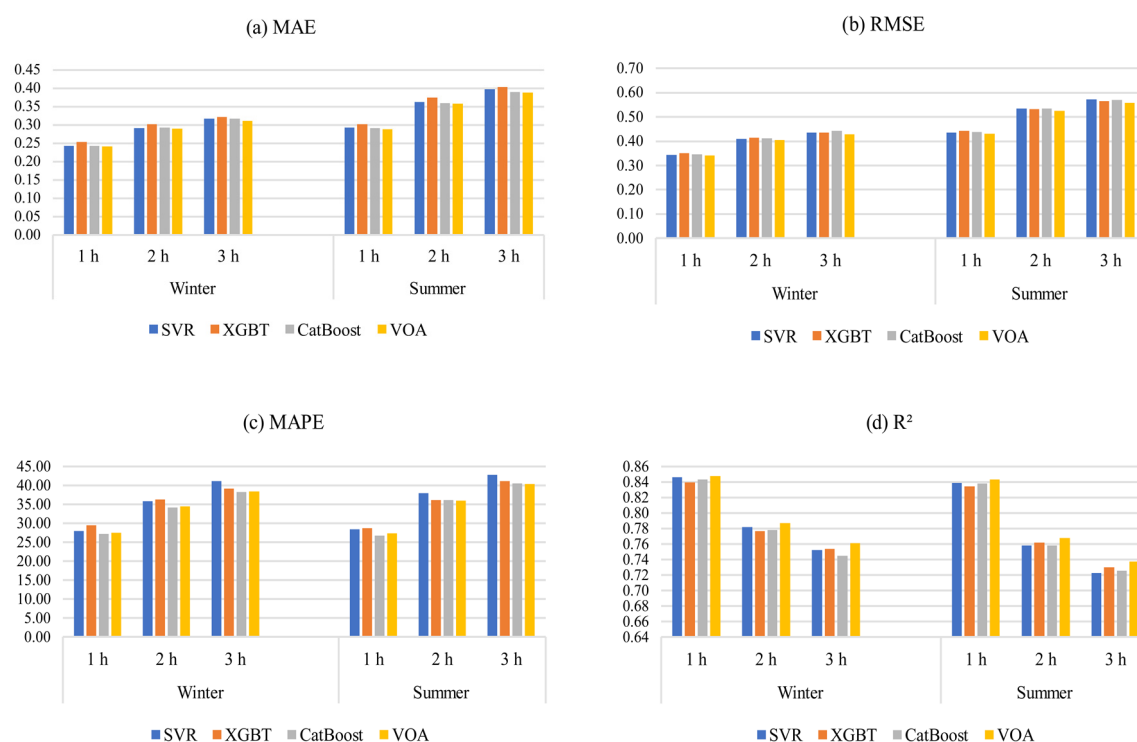


Figure 10. Performance of ML algorithms for different prediction time horizons: (a) MAE, (b) RMSE, (c) MAPE, (d) R^2 .

As expected, as the prediction horizon increases, forecasting errors increase and R^2 decreases, indicating the algorithm prediction performance degradation. Overall, the VOA demonstrated the best prediction performance among all ML algorithms used, outperforming other models in every prediction horizon, except for MAPE, wherein Catboost had the lowest error for all forecasting horizons. In most cases, XGBT presented the worst performance for a short prediction horizon (1 h), while SVR presented the worst performance for a longer prediction horizon (3 h).

Figure 11 shows the histogram and boxplot of absolute errors obtained when using VOA for the 1 h ahead and 3 h ahead forecasts. In the boxplot, the lower and upper lines denote the first and third quartile values (25th and 75th percentiles), respectively, and the median value (50th percentile) is represented by the central line. The lower and upper horizontal lines are the smallest and largest non-outliers, respectively, and outliers are represented by the '+' symbol. Results show that, as the prediction horizon increases, the error distribution tail becomes fatter, and the range of error values increases. It can be concluded that the proposed methodology results in acceptable forecasting errors up to 3 h ahead, with a maximum error of 0.31 (MAE) achieved by VOA.

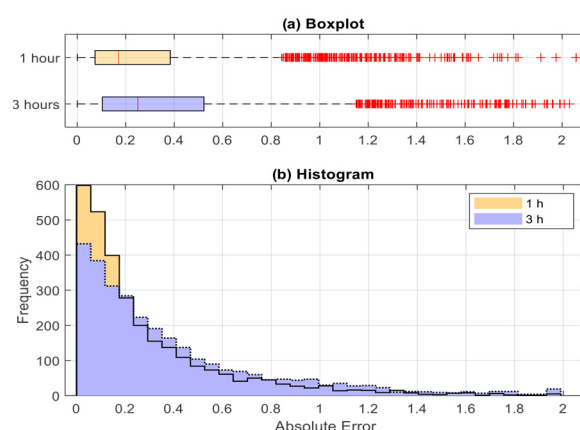


Figure 11. Absolute error using VOA to forecast 1 h ahead and 3 h ahead: (a) histogram and (b) boxplot.

This study presented promising results with the proposed forecasting methodology. However, it is important to mention that, if another database from a different location needs to be used, the same methodology should be applied, but simulations must be performed to adjust the hyperparameter of the ML algorithms.

6. Conclusions

In this paper, a solar forecasting methodology is proposed using machine learning algorithms and an ensemble feature selection method. The ensemble feature selection is used to choose the most related endogenous and exogenous inputs and their past observation values and integrates Pearson's coefficient, mutual information, random forest and relief. The advantage of the proposed feature selection method was validated comparing the obtained results against two other cases: (a) when only endogenous inputs are used and (b) when both endogenous and exogenous inputs are used, selected with Pearson's correlation coefficient. Four state-of-the-art ML algorithms were tested to forecast solar radiation, namely SVR, XGBT, CatBoost and VOA. The performance of these algorithms was evaluated using widely adopted statistical parameters, such as MAE, RMSE, MAPE, R^2 , skewness and kurtosis. Three prediction time horizons were considered: 1 h, 2 h and 3 h ahead.

This study did not aim to improve the accuracy of the machine learning models used (SVR, XGBT, CatBoost and VOA) but rather to evaluate and compare their performance using different sets of inputs. The forecast methodology proposed in the present research differs from the literature by using an ensemble feature selection for choosing past observation values of both endogenous and exogenous inputs.

The main results and conclusions are summarized below:

- The proposed ensemble feature selection outperformed the other two cases analyzed, one using only endogenous variables as inputs and the other using endogenous and exogenous variables as inputs, selected with Pearson's correlation coefficient;
- As the prediction horizon increased, the error distribution tail became fatter and the range of error values increased;
- All investigated machine learning models revealed acceptable forecasting performance. Among all algorithms, VOA offered the best predictive performance, outperforming other models in every prediction horizon, except for MAPE, wherein Catboost had the lowest error for all forecasting horizons;
- All algorithms have an acceptable testing speed for real-world applications, with an average execution computational time of 11 s. XGBT had a lower training speed, and VOA had a higher training speed.

- One interesting finding of this research was that forecasting error was larger in summer than in winter, since the algorithms used are sensitive to the database.

In this study, the maximum number of past observations adopted in the ensemble feature selection method was chosen empirically. The results and conclusions obtained suggest that more research should be carried out for the optimal selection of this parameter, aiming to attain more accurate forecasts. Finally, as the performance of ML algorithms mainly depends on the dataset used, more experiments can be investigated using different datasets from other locations than Brazil. Besides, the proposed methodology can be applied to other forecasting problems, such as wind speed and load forecasting.

Author Contributions: Conceptualization, C.M.A. and E.S.S.; methodology, C.M.A.; software, E.S.S.; validation, C.M.A. and P.D.; formal analysis, C.M.A.; investigation, C.M.A. and E.S.S.; resources, E.S.S.; data curation, E.S.S.; writing—original draft preparation, C.M.A.; writing—review and editing, E.S.S. and P.D.; visualization, E.S.S.; supervision, C.M.A.; project administration, C.M.A.; funding acquisition, C.M.A. All authors have read and agreed to the published version of the manuscript.

Funding: This research was supported by PROPESP/UFGA and CNPq, Brazil.

Data Availability Statement: Not applicable.

Conflicts of Interest: The authors declare no conflict of interest.

References

- IRENA. Renewable Capacity Highlights 2022. Available online: <https://www.irena.org/publications/2022/Apr/Renewable-Capacity-Statistics-2022> (accessed on 20 April 2022).
- Liu, C.; Li, M.; Yu, Y.; Wu, Z.; Gong, H.; Cheng, F. A Review of Multitemporal and Multispatial Scales Photovoltaic Forecasting Methods. *IEEE Access* **2022**, *10*, 35073–35093. <https://doi.org/10.1109/ACCESS.2022.3162206>.
- Larson, V.E. Forecasting Solar Irradiance with Numerical Weather Prediction Models. In *Solar Energy Forecasting and Resource Assessment*; Academic Press: Boston, MA, USA, 2013; pp. 299–318.
- Colak, I.; Yesilbudak, M.; Genc, N.; Bayindir, R. Multi-Period Prediction of Solar Radiation Using ARMA and ARIMA Models. In Proceedings of the 2015 IEEE 14th International Conference on Machine Learning and Applications (ICMLA), IEEE, Miami, FL, USA, 9–11 December 2015; pp. 1045–1049.
- Huang, J.; Korolkiewicz, M.; Agrawal, M.; Boland, J. Forecasting Solar Radiation on an Hourly Time Scale Using a Coupled AutoRegressive and Dynamical System (CARDS) Model. *Solar Energy* **2013**, *87*, 136–149. [doi:10.1016/j.solener.2012.10.012](https://doi.org/10.1016/j.solener.2012.10.012).
- Yadav, A.K.; Chandel, S.S. Solar Radiation Prediction Using Artificial Neural Network Techniques: A Review. *Renew. Sustain. Energy Rev.* **2014**, *33*, 772–781. <https://doi.org/10.1016/j.rser.2013.08.055>.
- Kumar, R.; Aggarwal, R.K.; Sharma, J.D. Comparison of Regression and Artificial Neural Network Models for Estimation of Global Solar Radiations. *Renew. Energy Rev.* **2015**, *52*, 1294–1299. <https://doi.org/10.1016/j.rser.2015.08.021>.
- Pedro, H.T.C.; Coimbra, C.F.M. Assessment of Forecasting Techniques for Solar Power Production with No Exogenous Inputs. *Sol. Energy* **2012**, *86*, 2017–2028. <https://doi.org/10.1016/j.solener.2012.04.004>.
- Dong, Z.; Yang, D.; Reindl, T.; Walsh, W.M. A Novel Hybrid Approach Based on Self-Organizing Maps, Support Vector Regression and Particle Swarm Optimization to Forecast Solar Irradiance. *Energy* **2015**, *82*, 570–577. <https://doi.org/10.1016/j.energy.2015.01.066>.
- Voyant, C.; Notton, G.; Kalogirou, S.; Nivet, M.-L.; Paoli, C.; Motte, F.; Fouilloy, A. Machine Learning Methods for Solar Radiation Forecasting: A Review. *Renew. Energy* **2017**, *105*, 569–582. <https://doi.org/10.1016/j.renene.2016.12.095>.
- Rodríguez, F.; Azcárate, I.; Vadillo, J.; Galarza, A. Forecasting Intra-Hour Solar Photovoltaic Energy by Assembling Wavelet Based Time-Frequency Analysis with Deep Learning Neural Networks. *Int. J. Electr. Power Energy Syst.* **2022**, *137*, 107777. <https://doi.org/10.1016/j.ijepes.2021.107777>.
- Elizabeth Michael, N.; Mishra, M.; Hasan, S.; Al-Durra, A. Short-Term Solar Power Predicting Model Based on Multi-Step CNN Stacked LSTM Technique. *Energies* **2022**, *15*, 2150. <https://doi.org/10.3390/en15062150>.
- Boubaker, S.; Benghanem, M.; Mellit, A.; Lefza, A.; Kahouli, O.; Kolsi, L. Deep Neural Networks for Predicting Solar Radiation at Hail Region, Saudi Arabia. *IEEE Access* **2021**, *9*, 36719–36729. <https://doi.org/10.1109/ACCESS.2021.3062205>.
- Wentz, V.H.; Maciel, J.N.; Gimenez Ledesma, J.J.; Ando Junior, O.H. Solar Irradiance Forecasting to Short-Term PV Power: Accuracy Comparison of ANN and LSTM Models. *Energies* **2022**, *15*, 2457. <https://doi.org/10.3390/en15072457>.
- Massaoudi, M.; Abu-Rub, H.; Refaat, S.S.; Trabelsi, M.; Chihi, I.; Oueslati, F.S. Enhanced Deep Belief Network Based on Ensemble Learning and Tree-Structured of Parzen Estimators: An Optimal Photovoltaic Power Forecasting Method. *IEEE Access* **2021**, *9*, 150330–150344. <https://doi.org/10.1109/ACCESS.2021.3125895>.
- Mahmud, K.; Azam, S.; Karim, A.; Zobaed, S.; Shanmugam, B.; Mathur, D. Machine Learning Based PV Power Generation Forecasting in Alice Springs. *IEEE Access* **2021**, *9*, 46117–46128. <https://doi.org/10.1109/ACCESS.2021.3066494>.

17. Castangia, M.; Aliberti, A.; Bottaccioli, L.; Macii, E.; Patti, E. A Compound of Feature Selection Techniques to Improve Solar Radiation Forecasting. *Expert Syst. Appl.* **2021**, *178*, 114979. <https://doi.org/10.1016/j.eswa.2021.114979>.
18. Tao, C.; Lu, J.; Lang, J.; Peng, X.; Cheng, K.; Duan, S. Short-Term Forecasting of Photovoltaic Power Generation Based on Feature Selection and Bias Compensation–LSTM Network. *Energies* **2021**, *14*, 3086. <https://doi.org/10.3390/en14113086>.
19. Surakhi, O.; Zaidan, M.A.; Fung, P.L.; Hossein Motlagh, N.; Serhan, S.; AlKhanafseh, M.; Ghoniem, R.M.; Hussein, T. Time-Lag Selection for Time-Series Forecasting Using Neural Network and Heuristic Algorithm. *Electronics* **2021**, *10*, 2518. <https://doi.org/10.3390/electronics10202518>.
20. INMET. Instituto Nacional de Meteorologia. Available online: <https://portal.inmet.gov.br/> (accessed on 23 October 2021).
21. Han, J.; Kamber, M.; Pei, J. *Data Mining: Concepts and Techniques*, 3rd ed.; Elsevier Inc.: Waltham, MA, USA, 2012.
22. Mera-Gaona, M.; López, D.M.; Vargas-Canas, R.; Neumann, U. Framework for the Ensemble of Feature Selection Methods. *Appl. Sci.* **2021**, *11*, 8122. <https://doi.org/10.3390/app11178122>.
23. Shannon, C. A mathematical theory of communication. *Bell Syst. Tech. J.* **1948**, *27*, 379–423. <https://doi.org/10.1002/j.1538-7305.1948.tb01338.x>.
24. Breiman, L. Random forests. *Mach. Learn.* **2001**, *45*, 5–32. <https://doi.org/10.1023/A:1010933404324>.
25. Kira, K.; Rendell, L. A Practical Approach to Feature Selection. *Mach. Learn. Proc.* **1992**, *1992*, 249–256. <https://doi.org/10.1016/B978-1-55860-247-2.50037-1>.
26. Shalev-Shwartz, S.; Ben-David, S. *Understanding Machine Learning: From Theory to Algorithms*, 1st ed.; Cambridge University Press: New York, NY, USA, 2014.
27. Chen, T.; Guestrin, C. XGBoost: A Scalable Tree Boosting System. In Proceedings of the 22nd ACM SIGKDD International Conference on Knowledge Discovery and Data Mining, San Francisco, CA, USA, 13–17 August 2016.
28. Prokhorenkova, L.; Gusev, G.; Vorobev, A.; Dorogush, A.; Gulin, A. CatBoost: Unbiased boosting with categorical features. In Proceedings of the 32nd International Conference on Neural Information Processing Systems, Montréal, QC, Canada, 3 December 2018.
29. An, K.; Meng, J. Voting-Averaged Combination Method for Regressor Ensemble. In *Advanced Intelligent Computing Theories and Applications*; Huang, D.S., Zhao, Z., Bevilacqua, V., Figueroa, J.C., Eds.; Springer: Berlin/Heidelberg Germany, 2010; Volume 6215, pp. 540–546.
30. Agrawal, T. Hyperparameter Optimization Using Scikit-Learn. In *Hyperparameter Optimization in Machine Learning*; Apress: Berkeley, CA, USA, 2021; pp. 31–51. ISBN 978-1-4842-6578-9.